



1 **Geometry and topology of Polish Outer Carpathian digital**
2 **elevation model interpreted lineament network in context of**
3 **regional tectonics**

4 Maciej Kania¹, Mateusz Szczęch¹

5 ¹Jagiellonian University in Kraków, Faculty of Geography and Geology, Institute of Geological Sciences,
6 Gronostajowa 3a, 30-863 Kraków, Poland

7 *Correspondence to:* Maciej Kania (maciej.kania@uj.edu.pl)

8



9 **Abstract.** The Polish part of the Western Outer Carpathians lineament network was analysed based on the
10 GMTED2010 digital elevation model. Lineaments were identified in the visual screening of the hillshade model.
11 To the best of our knowledge, no one has studied the geometrical properties of the network with relation to the
12 topological ones. The NetworkGT QGIS toolbox was applied to identify the nodes and branches of the network,
13 as well as to calculate the topology parameters. Our aim was to find differences between the western and eastern
14 parts of the Western Outer Carpathians; therefore, the analyses were carried out in six sectors chosen based on
15 the geographical subdivision in the geological context: three in the north, mainly the Silesian unit; and three in
16 the south, mainly the Magura unit. We found general agreement of the identified network with the
17 photolineament map; however, some of the photolineaments are not confirmed by digital elevation model
18 (DEM). We found that the topological parameters of the networks change from west to east, but not from north
19 to south. There are areas of increased interconnectivity, especially the Nowy Sącz Basin, where the lineament
20 network may reflect a complicated system of cross-cutting deep-rooted fault zones in the basement.

21 1. Introduction

22 Remote sensing imagery is an important source of data in regional tectonics, and its importance has been growing
23 in recent years. Since the 1970s, there have been multispectral satellite photos of the Earth surface applied mainly
24 in mineral mapping (e.g. van der Meer et al., 2012), as well as in tectonic studies (e.g. Leech et al., 2003). The
25 Shuttle Radar Topography Mission (SRTM) resulted in the first remote sensing digital elevation model of most of
26 the continental surface of the planet, with immense potential for application in geology (Yang et al., 2011). Then,
27 new superior resolution and quality models were created on both the global (satellite) and local scale (mainly
28 airborne LiDAR scanning). Digital elevation models are especially useful in areas with lush vegetation. The
29 application of LiDAR in the Carpathians' flysch-type mountains in geological interpretations was shown, for
30 example, in Kania and Szczęch (2022).

31 Our previous study (Kania and Szczęch, 2020), based on the interpretation of the model augmented with field
32 geological mapping (Szczęch and Cieszkowski, 2021), showed how a lineament network can be interpreted in
33 topological and geometrical terms. The aim in the present paper is to up-scale DEM-based geometrical and
34 topological analyses of a regional scale lineament network to find how this is reflected in the tectonic structure of
35 the Western Carpathians. Previous studies of the Carpathian lineaments were mainly focused on lineament strikes
36 distribution (e.g. Doktor and Graniczny, 1982, 1983; Doktor et al., 1985, 1990, 2002; Bażyński et al., 1986;
37 Graniczny and Mizerski, 2003); therefore, we decided to add an interconnectivity aspect in terms of the topological
38 parameters (Valentini et al., 2007; Sanderson and Nixon, 2015; Thiele et al., 2016), as a way of better
39 understanding the structural problems. Most of the Carpathian-related studies are geographically organised in
40 mountain arc parallel belts, reflecting the main tectonostratigraphic units, now forming nappes and being
41 sedimentary basins during the Carpathian flysch depositions. We decided to keep this subdivision, although
42 combining this with physiographical subdivisions into sectors with borders perpendicular to the Carpathian belt.

43 2. Up-to-date research on the Polish Outer Carpathian lineaments

44 The fact that dislocation lines perpendicular to the Carpathian arc are related to the deep basement, and are
45 significantly older than the Carpathians themselves, was postulated even before the remote sensing era (Teisseyre,
46 1907). The first modern attempts to interpret lineaments in the Polish Carpathians were based on the Landsat MSS
47 imagery and Heat Capacity Mapping Mission satellite, and reported together with data from the whole territory of



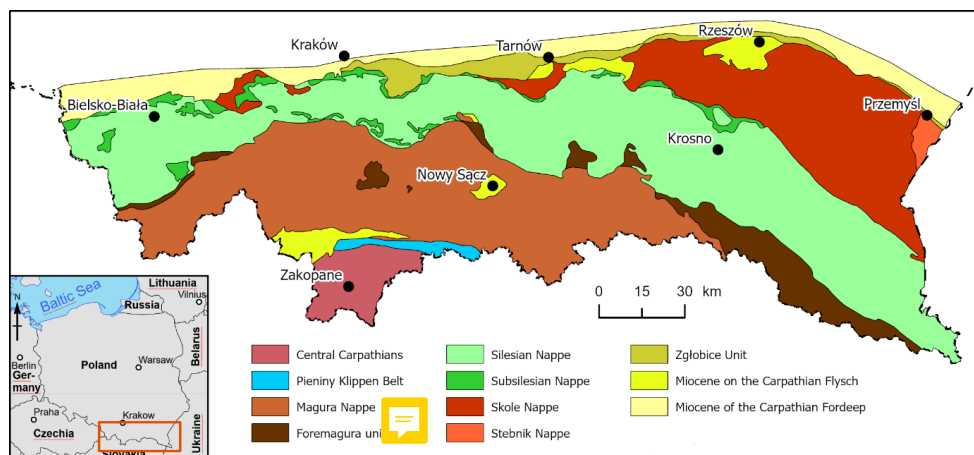
48 Poland on a photogeological map at 1:1 000 000 scale (Graniczny and Mizerski, 2000; Bażyński et al., 1986). The
49 main lineament systems of the Western Carpathians in the context of structural geology were shown by Doktor
50 and Graniczny (1983) and Doktor et al. (1985). The results of satellite imagery lineament detections were then
51 correlated with geophysical data proving relationships between the surface, neotectonic processes and deep
52 Carpathian basement structure (Doktor et al., 1990; Motyl-Rakowska and Ślącza, 1984). Airborne radar data
53 were applied in tectonic analysis of the Carpathians, resulting in 17 000 short lineaments that were the basis of the
54 lineament density map (Doktor et al., 2002). The interpretation of SRTM hillshading visualisation was performed
55 by Chodyń (2004) on the limited area in Beskid Wyspowy Mts. Comparison of Landsat MSS and SRTM data by
56 Ozimkowski (2008) showed that whilst the main faults can be related to lineaments, there are still numerous
57 lineaments without geological explanation.

58 3. Study area

59 The choice of the study area was based on the physiogeographical subdivision of Poland by Solon et al. (2018).
60 The following macroregions were selected: the Western Beskidy Foothills, Western Beskidy Mts., Orawa–Podhale
61 Basin, Mid-Beskidy Foothills and Mid-Beskidy Mts. These five regions, with a total area of 17 437 km², cover
62 most of the Polish part of the Outer Carpathians, excluding a small part of the Eastern Outer Carpathians located
63 in Poland.

66 3.1 Geological setting of the study area

67 The research area is located in the Polish sector of the Western Outer Carpathians (Mahel', 1974; Książkiewicz,
68 1977; Ślącza et al., 2006; Fig. 1). It contacts tectonically with the Pieniny Klippen Belt from the south, which is
69 a border between the Outer and the Central Carpathians (Plašienka, 2018; Golonka et al., 2019a, 2019b;
70 Książkiewicz, 1977). The Outer Carpathians are built mainly of flysch deposits, whose thickness is approximately
71 6 000 m, and thus they are also referred to as the Flysch Carpathians (Golonka et al., 2020; Ślącza et al., 2006;
72 Golonka et al., 2005; Książkiewicz, 1977). These deposits are Late Jurassic–Early Miocene in age and are mainly
73 deep-sea sediments deposited by the gravity flow in the several sedimentary basins of the Northern Tethyan
74 separated by ridges (Golonka et al., 2005, 2020; Ślącza et al., 2006; Książkiewicz, 1977). The thrust of the Central
75 Carpathians block to the north on the European platform blocks — the Brunovistulicum and Małopolska Massif
76 (Żaba, 1999) — led to the forming of the synorogenic stage accretionary prism. The sediments deposited in the
77 basins were folded and thrust one upon another, creating the sequence of the nappes in the Miocene. Going from
78 the south there are the Macura Nappe, Doktor Nappe, Fore–Magura group of nappes, Silesian Nappe, Sub-Silesian
79 Nappe and Skole Nappe (Mahel', 1974; Książkiewicz, 1977; Golonka et al., 2005, 2019a; Ślącza et al., 2006).
80 The deposits of the Outer Carpathians are overlain on the Miocene molasses filling the Carpathian Foredeep,
81 which was deposited on the front of the Outer Carpathian orogenic belt thrusting over the North European
82 Platform (Ślącza et al., 2006; Oszczytko, 2006).

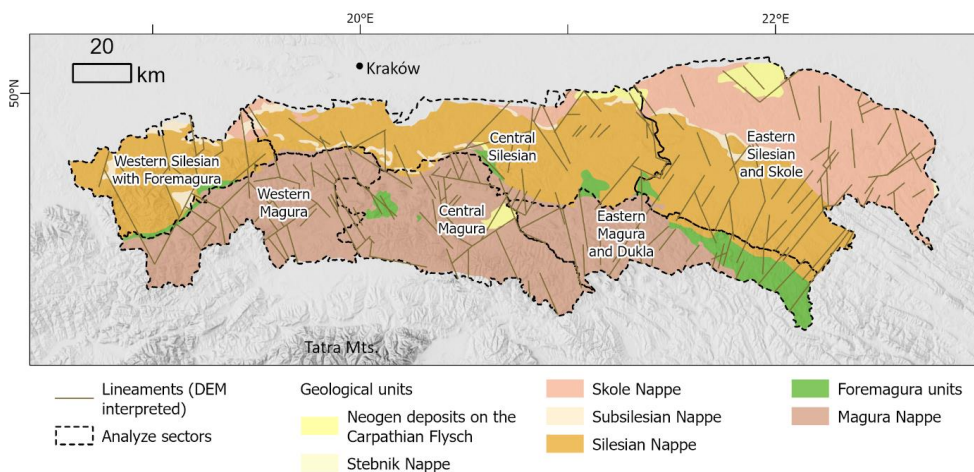


83
84
85
86

Fig. 1. Generalised geological map of the Polish part of the Carpathians based on Cieszkowski et al., 2017 and cited there.

87 3.2 Analysis of the sectors

88 We used the morphometry subdivision of Poland (Solon et al., 2018) to define the area, based on the subprovinces
89 of the Western Outer Carpathians in the area of Poland and a small band of Northern Subcarpathia subprovince to
90 the border of the Carpathians in the geological meaning (Carpathian overthrust on the Foredeep sediments),
91 according to Lexa et al. (2000). The subdivision of the outer Carpathian belt is mostly used in the geology basis
92 on the tectonostratigraphic units (nappes). This subdivision, however, does not allow differences in lineament
93 systems parallel to the belt to be caught. The newly proposed morphostructural subdivision of the Western
94 Carpathians (Minár et al., 2011) is another approach that compiles geological and morphological features. The
95 Polish part of the Western Carpathians is subdivided into the following subregions (number according to the paper
96 cited): (3f) Moravian–Silesian Beskid, (3a) Beskid Żywiecki–Gorce, (3b) Beskid Sądecki–Levočské vrchy, (5a)
97 Beskid Wyspowy, (5b) Low Beskid and (6) North Foreland. The last subregion spans all the length of the northern
98 Carpathian boundary between the Orava and San rivers. We decided to compile the geological subdivision with
99 the morphological one (Solon et al., 2018), which also comprises a subdivision of the outermost units, into five
100 sectors (Fig. 2, Tab. 1). The only change was including Ciecierzyn in Beskid Wyspowy into the Central
101 Silesian sectors, as this massif, unlike all other Beskid Wyspowy culminations is built of Silesian series deposits



102

103

Fig. 2. Sectors defined based on the physiogeographical (Solon et al., 2018) and tectonic subdivisions (Golonka et al., 2020) of the study area (Western Outer Carpathians in Poland).

104

105

106

Tab. 1. Analyse sectors

Analyse sectors name;	Symbol	Mesoregions covered according to Solon et al., 2018
Western Silesian with Foremagura	WS	Silesian Beskid Mts., Żywiec Basin, Silesia Foothills, Mały Beskid Mts.
Central Silesian	CS	Wieliczka Foothills, Wiśnicz Foothills, Beskid Wyspowy Mts – only the Ciecień ridge, Rożnow Foothills, Ciężkowice Foothills, Gorlice Basin
Eastern Silesian and Skole	ES	Przemyśl Foothills, Jasło-Krosno Basin, Strzyżów Foothills, Dynów Foothills, Jasło Foothills, Bukowiec Foothills
Western Magura	WM	Orawa-Jordanów Foothills, Orawa Interfluve, Koniaków Intermontane Region, Żywiec-Kysuce Beski, Pewel-Krzeczów Ranges, Makowski Beskid, Żywiec-Orawa Beskid
Central Magura	CM	Sącz Beskid Mts., Sącz Basin, Wyspowy Beskid (without Ciecień Ridge), Gorce Mts.
Eastern Magura and Dukla	EM	Low Beskid Mts.

107

108 4. Data and methods

109 4.1 Digital elevation model

110 The Global Multi-resolution Terrain Elevation Data 2010 (GMTED2010; see Danielson, 2011) 7.5 arc-second
 111 product was chosen as a work base. The model is a compilation of different raster-based elevation sources, based



112 mainly on SRTM digital terrain elevation data. The resolution is ca. $0.0021^\circ/\text{pixel}$, which means ca. 233 m/pixel.
113 This was found to be sufficient, while the working scale during lineament detection was 1:150 000. As the shading
114 azimuth can influence the results, the working imagery was multidirectional hillshade (Introducing the Next
115 Generation Hillshade, 2022).

116 **4.2 Multiple cover lineament detection**

117 The manual method of lineament extraction was applied for two reasons. First, it is the simplest, low cost and
118 widely used method. The second reason is that it creates a basis for further work, based on automated extraction.
119 However, the method used is prone to some operator-related bias (Scheiber et al., 2015; Ehlen, 2004). Thus, to
120 reduce this bias the lineaments were extracted by two operators working independently, in three sessions, separated
121 by intervals of several months. After each session, the results were analysed and a network of common features
122 was created. The last stage was creating a concise network of lineaments based on the results of the three sessions.
123

124 **4.3 Network analysis**

125 A network can be described by scale-independent topological characteristics, based on the case of a line network
126 on graph theory. The network (graph) is formed by nodes (end or intersection points) connected by lines
127 (Sanderson and Nixon, 2015; Mukherjee, 2019). The line can be formed by one or more branches connected by
128 nodes. The node can be isolated (I type), an embranchment (Y type) or an intersection (X type), where the latter
129 two types are connecting nodes. Thus, the branch can connect two I type nodes (I–I branch), isolated and
130 connecting nodes (I–C branch, which can be I–Y or I–X) and two connecting nodes (C–C branch, which can be
131 X–X, X–Y or Y–Y). The proportion of nodes and branch types can be analysed as tertiary systems that characterise
132 the properties of the network, especially its interconnectivity (Procter and Sanderson, 2018; Sanderson and Nixon,
133 2015; Sanderson et al., 2018).

134 The spatial variation of the topological parameters of the network was analysed with the following aspects: (1)
135 regular, in a 5x5 km grid; and (2) within sectors based on the mesoregions of physiogeographical subdivision,
136 according to Solon et al. (2018) and the main tectonic units (Fig. 2 Tab. 1).

137 The NetworkGT QGis toolbox (Nyberg et al., 2018) was used as a tool in the topological analyses. The lineament
138 network was checked and repaired with NetworkGT tools. An additional stage was the manual correction of some
139 features to eliminate all non-defined types of nodes, as well as some extremely short (ca. 500 m or shorter) features.
140 The topological parameters were analysed in three modes: the whole network; the sectors defined; and in a regular,
141 5x5 km grid with 10 km search radius.

142 The Rayleigh test of semicircular distribution test was performed with the EZ-ROSE spreadsheet (Baas, 2000),
143 and circular statistics were calculated with the SciPy stats module (The SciPy Community, 2022).

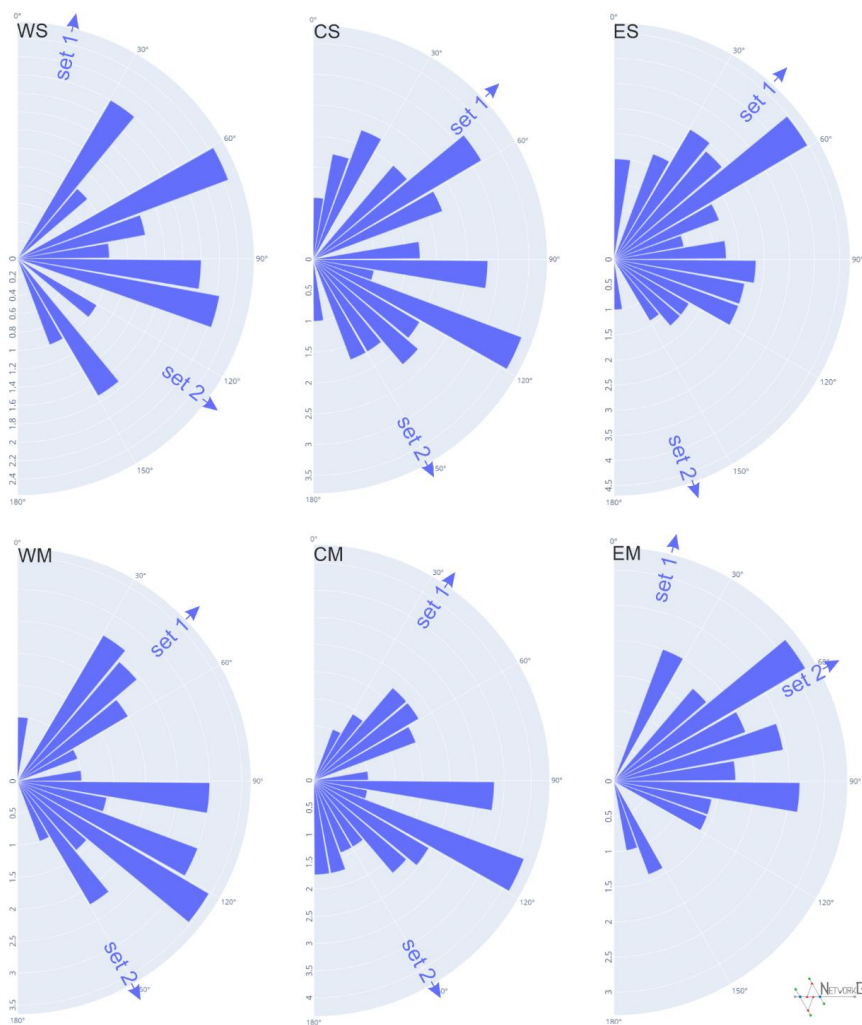
144 **5. Results**

145 **5.1 Network geometry**

146 The azimuths of the lineaments in all the analysed sectors show a multimodal distribution. Thus, the directions
147 were separated into sets, in a way that gives low values of circular variance. The angular ranges of all the sets are
148 presented in Tab. 2. For all sets, except for set 2 in the Eastern Magura (EM) sector and set 2 in the Western



149 Silesian (WS) sector, the distribution is not uniform, as checked with the Rayleigh test (Baas, 2000). The two sets
 150 not checked were not numerous enough to be representative.



151
 152 **Fig. 3:** Rose diagrams of the analysed networks in the analytic sectors; upper row: Western Silesia with
 153 Foremagura (WS), Central Silesia (CS), Eastern Silesia (ES); lower row: Western Magura (WM), Central
 154 Magura (CM), and Eastern Magura (EM). Arrows mark the mean azimuth for the sets defined in Tab. 2.

155
 156 **Tab. 2.** Azimuths of the lineaments in the analyse sectors

Analyse sector	Set	Azimuths range	n	Circular statistics			The acute angle between sets means
				Mean	Std. dev	Variance	
CS	1	0 – 100	15	46.5	14.2	3.5	75.5
	2	100 – 180	13	151	16.6	4.8	



CM	1	0 – 80	17	34.1	13	3	63.9
	2	80 – 180	51	150.2	21.5	8.1	
EM	1	45 – 75	41	62.1	7.5	1.0	47.7
	2	0 – 45 75 – 180	3	14.4	26.7	12.5	
ES	1	0 – 100	59	42.7	19.7	6.8	62.1
	2	100 – 180	28	160.6	14.7	3.8	
WM	1	0 – 100	20	46.5	14.2	3.5	75.5
	2	100 – 180	40	151	16.6	4.8	
WS	1	0 – 60 150 – 180	23	13.6	23.3	9.5	66.2
	2	60 – 150	5	127.4	8.9	1.4	

157

158 The orientation of lineaments in all sectors, as well as the circular mean azimuth are shown in Fig. 3. In sectors
 159 Central and Eastern Silesian (CS, ES) and Central and Western Magura (CM, WM) the set 1 mean is located
 160 between 34° and 47°, marking a dominant SW–NE strike of lineaments. In the Western Silesian sector (WS), set
 161 1 is oriented more to the north (14°). In all sectors above, there is a second set with a NW–SE trend, mostly oriented
 162 at 150–160°, but in the Western Silesian sector case the mean azimuth is lower (127°), as in the case of the first
 163 set. The last sector, Eastern Magura and Dukla, is different. There is one dominant set with azimuth 62°, and the
 164 second set is poorly represented and oriented northward. The angle between the two sets varies in the 62–76°
 165 range, except in the Eastern Magura and Dukla sector where it is only 48°.

166 5.2 Network topology

167 In the study area, 305 lineaments were marked in total. These features comprise 432 nodes. Of this count, 58% are
 168 I nodes, 19% are E nodes, 18% are Y nodes and 5% are X nodes. The network contains 338 branches, within
 169 which 49% are C–I type branches, 29% are C–C branches and 22% are I–I branches marking completely separated
 170 lineaments. Topological parameters are shown in Tab. 3.

171

172 **Tab. 3. Topological parameters of the network in analyse sectors**

	Western Silesian with Foremagura	Central Silesian	Eastern Silesian and Skole	Western Magura	Central Magura	Eastern Magura and Dukla	Whole area
	WS	CS	ES	WM	CM	EM	
No. of nodes (I+X+Y)	19	68	101	47	67	40	383
I nodes	8	51	76	26	48	36	293
X nodes	1	6	6	3	6	2	19
Y nodes	10	11	21	18	15	2	71
E nodes	22	38	49	46	61	52	-



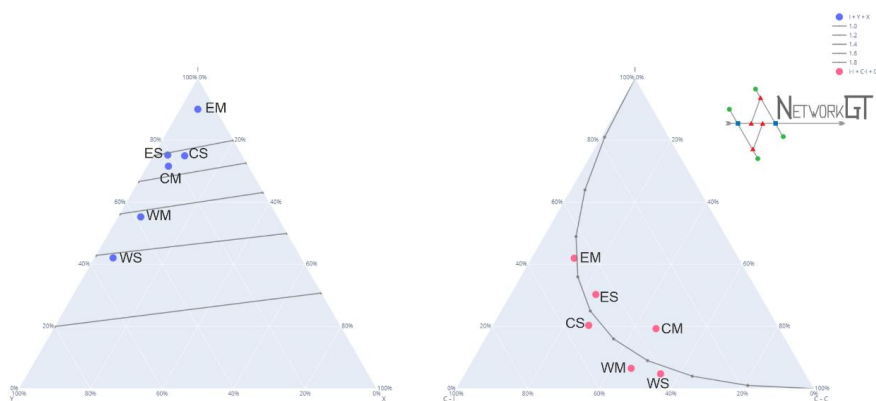
C-C connections	11.5	14.5	18.5	21.0	33.5	3.0	77.0
C-I connections	8.5	28.5	35.5	22.0	25.0	11.5	131.0
I-I connections	1.0	11.0	23.5	3.0	14.0	10.5	81.0
No. of branches	21.0	54.0	77.5	46.0	54.5	25.0	291
No. of lines	9.0	31.0	48.5	22.0	31.5	19.0	182
No. of connections	11	17	25	21	19	4	90
Connects per line	2.44	1.10	1.03	1.91	1.21	0.42	0.99
Connects per branch	1.62	1.06	1.02	1.43	1.12	0.56	0.99
Dim.less intensity	1.21	0.87	1.21	1.65	1.33	2.06	0.75
Av. degree of network	2.21	1.59	1.53	1.96	1.63	1.25	1.52

173

174

175 The highest dimensionless intensity parameter is in the Eastern Magura and Dukla sector (2.05) and the lowest in
 176 the Central Silesian (0.87). On the other hand, the Eastern Magura sector is characterised by the lowest connections
 177 per branch (0.56) or the average degree of network (1.25) due to its form of mainly parallel features, with only
 178 12% of the branches of connecting type (C–C). The best interconnectivity is observed in the Western Silesian
 179 sector with 1.62 connections per branch and an average degree of the network of 2.21. This is an effect of the
 180 presence of the Żywiec Basin block-system in the central part of the region.

181 The difference between these two (Eastern Magura and Western Silesia) sectors can be clearly visible on the
 182 ternary diagrams (Fig. 4) presenting the relationships of the nodes and branch types. In the Western Silesian sector,
 183 there is a high ratio of Y type nodes (52% of non-E-type nodes) and only one I–I branch.



184
185 **Fig. 4: Ternary diagram presenting nodes (left) and branches (right) proportions in the analyse sectors.**

186
187 The parameters of all the other sectors fall between the Eastern Magura and Western Silesian sectors. The Western
188 Magura sector has quite good interconnectivity with a similar type of Eastern Magura blocky network.

189 Another approach to analysing topology is to use a sampling regular grid. The results are shown in Fig. 4 as maps
190 of connections per branch number, 2D network intensity and dimensionless intensity.

191 It can be seen that in terms of connections per branch we have two relatively large regions with a high number
192 The first one is in the Western Silesian and partially Western Magura sectors, that is, the Żywiec Basin area, but
193 from the geological point of view it is also a narrow zone of foremagura units occurring between the Silesian and
194 Magura nappes. Moreover, the Subsilesian unit tectonic window occurs in this area.

195 The Nowy Sącz Basin (eastern part of the Central Magura sector in the subdivision used here) is the next region
196 with a high number of connections per network branch. The lineament system in this area surrounds a zone of
197 Neogene deposits lying on the Carpathian flysch and filling the intramountain Nowy Sącz Basin.

198 The 2D intensity map shows that the Nowy Sącz Basin is characterised in general by a higher intensity than the
199 Żywiec Basin. There is also a general trend of higher intensity in the western part of the Carpathians (especially
200 the Western Magura and Central Magura sectors) than in the eastern part (Eastern Magura and Dukła).

201 In terms of dimensionless intensity parameter there are two regions with significantly high values: the south-
202 eastern part of the Wiśnicz foothill, which is in the Central Silesian sector, and the eastern parts of the Beskid
203 Niski Mts. and Bukowiec foothill in the Eastern Magura and Eastern Silesian sectors, on the geographical border
204 of the Western and Eastern Carpathians.

205 6. Discussion

206 6.1 Different lineament identification approaches

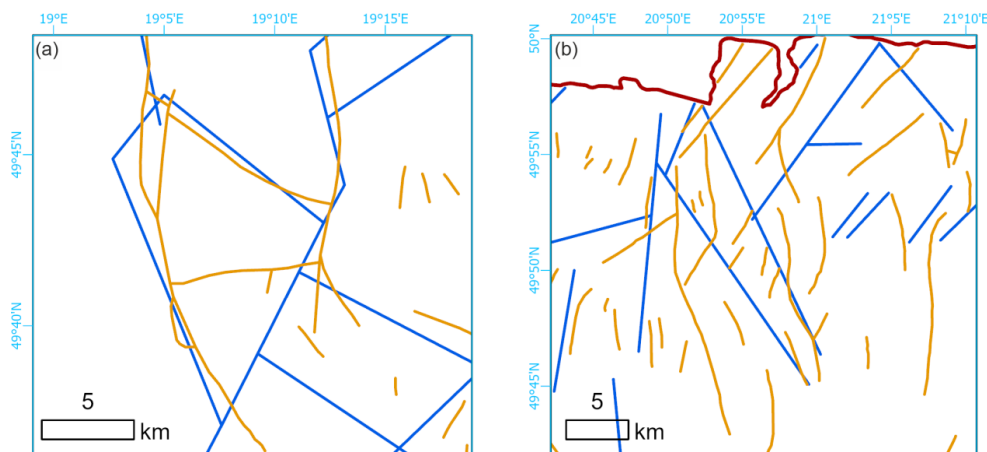
207 There are 110 photolineaments marked on the photogeological map of Poland in the studied area (Bażyński et
208 al., 1986). In the same area of the geological map of the Carpathians, Lexa et al. (2000) marked 2 325 features
209 described as a fault or assumed fault. In many cases, our lineament system seems to be concordant or
210 complementary to Lexa et al.'s (Fig. 5). In some cases, the features marked as faults are rather thrust lines, as per
211 the Fig. 5 example. The photolineament system is in general concordant with the DEM-interpreted system.

212 Visual inspection of the compiled lineaments map (Fig. 6a) shows that the especially NE striking lineaments of

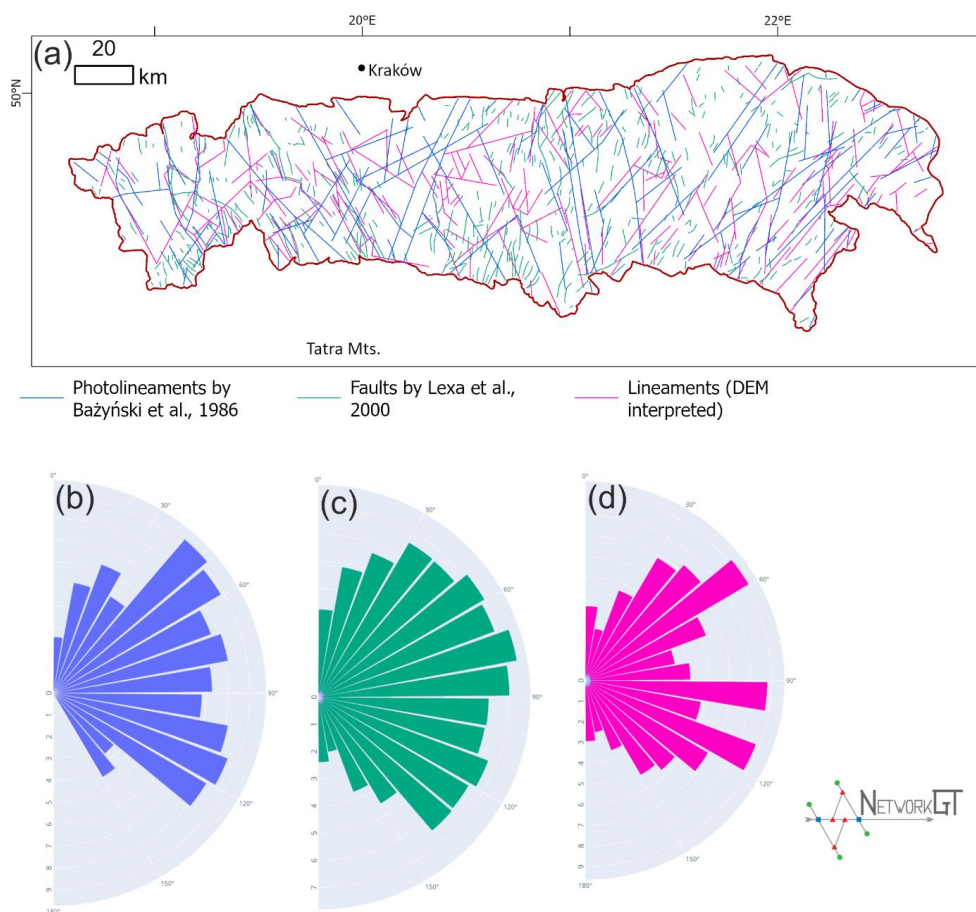


213 the Eastern Magura sector are consistent with each other. Moreover, the system framing the Żywiec tectonic
214 window is well visible in both sets. On the other hand, there are some photolineaments that are not recognisable
215 on the DEM, and in fact also hardly visible on the modern orthophoto map. The most prominent example are two
216 straight, parallel lineaments striking the NNE in the central part of the study area, cutting its entire width. These
217 features seem to cut Gorcze Mts.; this is not confirmed by our other studies (Kania and Szczęch, 2020; Szczęch
218 and Cieszkowski, 2021). Further to the north, these two lineaments are delimiting massifs of the Beskid
219 Wyspowsy Mts. (Mogieliica, Łopień). These massifs are in fact particularly visible on the aerial photo, as rather
220 isometric 'islands', and are formed by core parts of the synclines (Wójcik et al., 2009). On the other hand, some
221 lineament systems well visible in DEM are not marked on the photolineament map, as per the case of the system
222 north of the Nowy Sącz. That shows how these two methods can in fact be recognised as complementary
223 approaches to the lineaments' identification.

224 The system from the map by Lexa et al. (2000) shows confirmed and inferred faults, which is why it is not fully
225 compatible with lineaments; the lineaments, even when mainly tectonic related, are in fact a broader term (O'Leary
226 et al., 1976). Especially, these data, despite being a very rich collection of features are not applicable for topological
227 analyses: most of the features are short and isolated even when forming a network. Nevertheless, these data include
228 faults that are identified with geological criteria that are not visible in the remote sensing (at least at the scale
229 applied in this paper or by Bażyński et al., 1986 photolineament map. These data are augmenting each other, which
230 is highly visible in the Piwnicodrój area, where DEM interpreted that the NNW striking lineament along the
231 Poprad River Valley (not present in the photolineament set) is flanked with a set of N or NNE striking faults,
232 which we have not identified on the DEM.



233
234 **Fig. 5. Comparison of lineament system detected from the GMETD model (blue) and faults by Lexa et al.,**
235 **2000 (brown). (a) Żywiec Basin area, (b) fragment of the Zakliczyn – Olszyny fault zone.**



236

237 **Fig. 6. Geometry of lineament networks in the Carpathians. (a) compilation map of lineaments by Bażyński**
238 **et al., 1986, faults by Lexa et al., 2000 and lineaments interpreted from DEM in the presented paper. (b-d)**
239 **rosediagrams of features azimuth in the whole study area from: (b) Bażyński et al. (1986), (c) Lexa et al.,**
240 **2000 and (d) DEM interpreted.**

241

242 When analysing the distribution of feature azimuth for the whole study area (Fig. 6b-d), it can be noted that the
243 directions for the photolineament set (B) and DEM-interpreted set (D) are quite similar. What is noteworthy is the
244 lack of azimuths greater than 150° in the photo set, which are present (albeit in a minority) in the DEM set.
245 Furthermore, the photo set shows two maxima, at ca. 45° and 110°, whilst in the DEM set there are three maxima
246 at ca. 50°, 100° and 110°. However, the dominating directions are not in fact distributed uniformly along the W–
247 E span of the Polish Western Carpathians, which can be clearly seen in Fig. 6a where the domination of NE
248 directions in the eastern sectors can be noticed, as well as the presence of two main directions in the western and
249 central sectors.



250 **6.2 Dominating directions of the lineament network**

251 We observed a difference in dominating azimuths of lineaments between the western/central sectors (WS, WM,
252 CS, CM) and eastern sectors (ES, EM) of the study area. The first ones are characterised by two distinct sets of
253 lineaments (NNE or NE and SE), while the second has an SE set that is strongly reduced.

254 According to the general tectonic model of the Outer Carpathians (Unrug, 1980), the flysch deposits are cut by
255 set sinistral strike-slip fault zones. These fault zones are arranged in a fan-like shape along the arc of the
256 Carpathians, leading to the rotation of the set of nappes (Unrug, 1980; Graniczny and Mizerski, 2003). The
257 observed trend of increasing importance of the NE direction to the east is consistent with this model. However,
258 the more complicated geometry of the western part of the network may be related to the more complicated
259 system of the deep-rooted fault zones in this part (see further discussion below).

260 **6.3 Topological differentiation of the network**

261 There are no topological analyses of the lineament networks for the Outer Carpathians. Our previous article
262 (Kania and Szczęch, 2022) was focused on one mountain massif: Gorce Mts. From the tectonic point of view,
263 this massif is quite homogenous, being located in the one tectono-facial unit (Magura unit) with some subunits
264 within (Bystrica and Krynica subunits). Therefore, the paper focused mainly on different lithostratigraphic units,
265 showing how different types of lithology differ in topology terms.

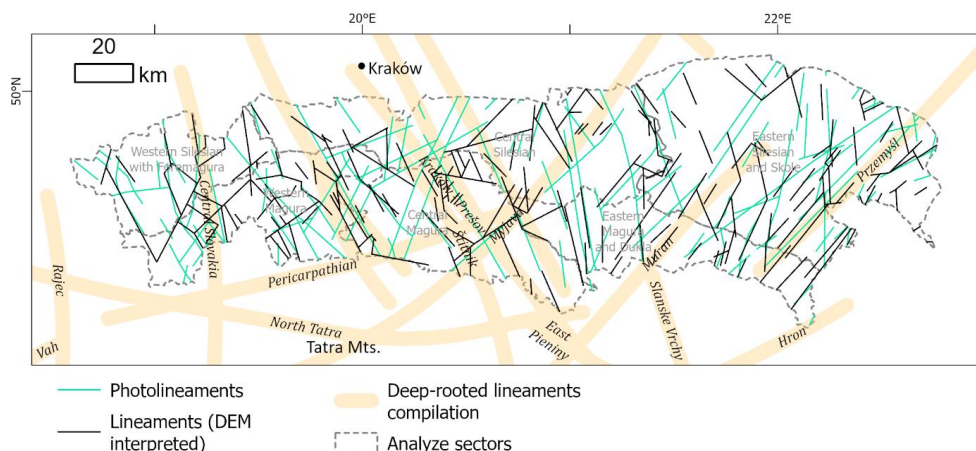
266 Scaling the research into the Polish Western Carpathians shows that in general there are no differences in the
267 network topology related to the tectono-facial units (Outer Carpathian nappes) since in general, all these units are
268 similar in lithology (flysch packets). However, there are differences related to some irregularities in tectonics:
269 especially, the intramountain basins are marked with increased network interconnectivity. The western part of the
270 study area in general has a better developed network. Especially, the Eastern Magura differs from the rest of the
271 sectors: the domination of one lineament direction results in low network interconnectivity, which is expressed by
272 a high proportion of the I nodes and I-I branches (Fig. 4). We analysed Magura unit and part of the Dukla unit
273 together; however, the interconnectivity in the Dukla Nappe (belonging to the Foremagura group) is stronger than
274 in Magura, which can be related to the proximity of the Silesian unit overthrust.

275 The highest interconnectivity was observed in the Western Silesian sector. The area is characterised by a high
276 proportion of Y nodes, and thus mainly by the presence of C-I or C-C branches (Fig. 4). In the geological
277 context, it is related to the location of the Żywiec tectonic window, which exposes the Subsilesian unit.

278 However, the topological study shows that the tectonised zone is wider; the increase in connections per branch
279 zone continues to the south along the Soła River and further, at least to the state border in the Beskid Żywiecki
280 Mts.

281 **6.4 Main large-scale, deep-rooted lineament systems of the Western Carpathians and their 282 relation to DEM-interpreted lineaments**

283 The following, well-known, large-scale lineaments reach the Carpathian basement cutting the Polish part of the
284 Outer Western Carpathians (Doktór et al., 1985): Central Slovakia, Myjava, Muran, Štitník and Przemyśl. There
285 are also lineaments not named by Doktór et al. (1985), but striking parallel, approximately 10 km to the east from
286 the Skawa fault zone (Cieszkowski et al., 2006). Fig. 7 presents the generalised positions of the lineaments.



287

288 **Fig. 7. Interpreted lineament system with photolineaments by Bażyński et al., 1986 as well as deep-rooted**
289 **lineament compilation after Sikora, 1976; Zuchiewicz, 1984; Doktór et al., 1985.**

290

291 The central Slovak line marks the eastern border of the Żywiec basin and marks the major fault zone well visible
292 in the displacing Fore–Magura belt near Żywiec. Some of the lineaments belonging to the system can also be
293 traced to the east, with some connecting NE–SW branches near the northern margin of the Carpathians.

294 The system of Muran lineaments in the discussed region is marked by a few short NE–SW lineaments in the eastern
295 sectors of the Magura and Silesian units. The Myjava system, in fact one of the most prominent systems in the
296 Carpathians, in the study area can be traced along the Nowy Sącz Basin, continuing to the north where there is a
297 series of short lines parallel to the zone lineaments. The network interconnectivity increases in this area. The
298 lineaments there lie in an extension of the Carpathian Shear Corridor, a large-scale strike–slip zone between Vienna
299 and the High Tatra Mts. (Marko et al., 2017). Although the Štitník system is unclear, some parallel or subparallel
300 lineaments can be assigned to this zone. The Przemysł lineament zone is identified as a set of long lineaments in
301 the easternmost parts of the area, where the main features of NE–SW are possibly interconnected by shorter N–S
302 lines, forming an interconnected, blocky, two-set system.

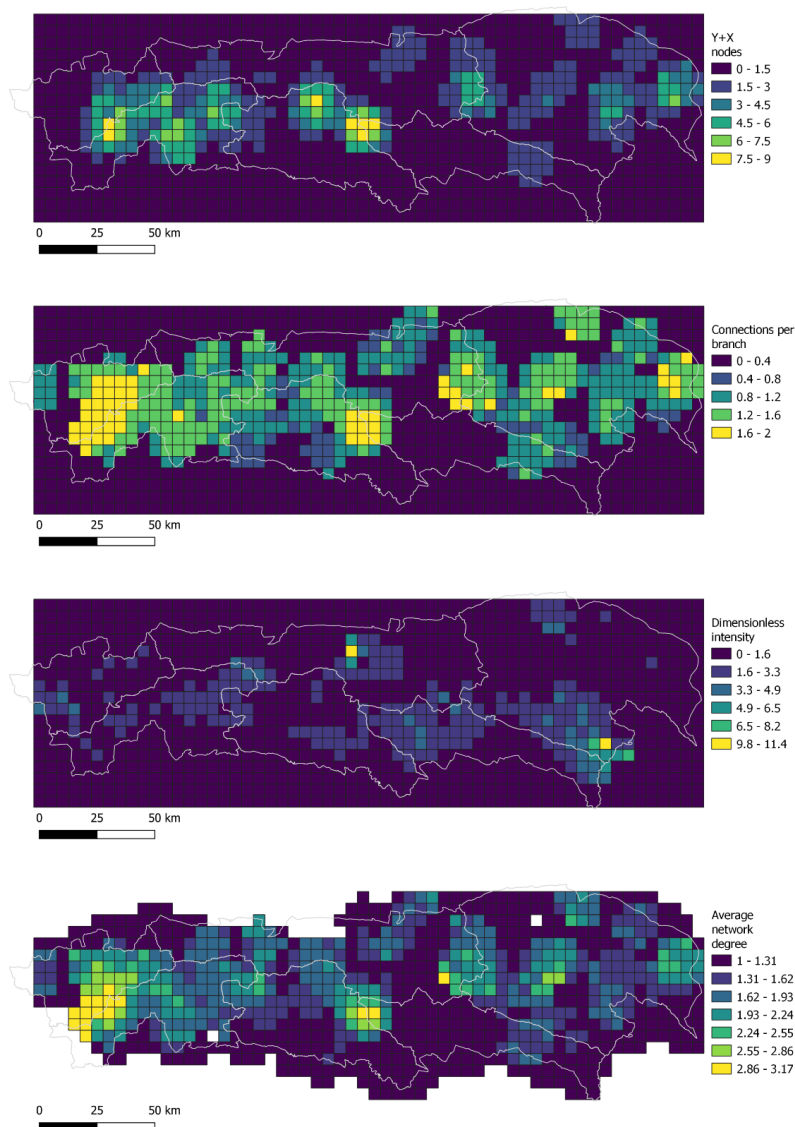
303 Another important deep-rooted linear structure, confirmed by a negative gravimetric anomaly is the Pericarpathian
304 line, which runs along the Nowy Sącz–Nowy Targ–Kysucké Nové Mesto line (Zuchiewicz, 1984; Sikora, 1976),
305 which runs similarly to the Myjava structure. The Kraków–Prešov lineament, which is an extension of the
306 Kraków–Lubliniec fault zone and marks the border between the Małopolska and Brunovistulicum blocks of the
307 basement (Žába, 1999; Zuchiewicz, 1984), runs along the Dunajec Valley. A system of lineaments is clearly visible
308 along this line, mainly in the Magura Nappe; however, parallel photolineaments were marked even longer to the
309 north (Bażyński et al., 1986).

310

311 These systems can be arranged in two sets: NNW, NW–SSE, SE striking (Central Slovakia, Skawa, Kraków–
312 Presov and Štitník); and NE–SE (Myjava and Pericarpathian, Muran and Przemysł). That implies some points of
313 system intersection, and in the area analysed such a place is in the Nowy Sącz region. This place is characterised
314 by higher interconnection factors (Fig. 8), in relation to the surrounding area. Moreover, in terms of



315 geomorphology, this is an intramountainous basin, being the only location where deposits are observed in the
316 Magura Nappe Neogene.



317
318

319 **Fig. 8. Topological parameters of the lineament network, from up to down: connections per branch number,**
320 **dimensionless intensity factor, and average network degree.**

321

322 The Central Slovakian system strikes along the east border of the Żywiec Basin and Żywiec tectonic window,
323 where the Subsilesian Nappe is exposed. We also marked a major lineament there, which is not present on the



324 photolineament map (Bażyński et al., 1986) or the database of the Western Carpathian Geological Map (Lexa et
325 al., 2000). The lineament (in the central part, the Soła River Valley) cuts the Magura Nappe, the Foremagura zone
326 with Magura overthrust and the Silesian Nappe. This structure is one of the edges of the rhomboidal block, in
327 which the Żywiec Basin has been developed. The generally increased degree of network interconnection (Fig. 8)
328 and the intensity of the network in this area can be an effect of the interaction between the central Slovakian system
329 with the Soła lineament and all the lowered block edges.

330 The cross-cutting relations of the Myjava lineament and the Stitnik lineament, whose continuation can be the
331 Dunajec fault system, are reflected in the bimodality of lineaments. The dominating maximum in the central
332 Magura sector, at approximately 120°, is similar to the Stitnik lineament; however, the Myjava lineament is
333 reflected there by just a few dominating lineaments, which are relatively long. Moreover, the Pericarpathian
334 lineaments are also known in this region. This structure, reflected in the sedimentary cover as the Dunajec fault
335 zone, is also confirmed by a negative gravimetric anomaly (Zuchiewicz, 1984; Sikora, 1976). Another deep
336 structure cutting this area is the Kraków–Presov fault, which is an extension of the Kraków–Lubliniec fault zone
337 under the Carpathians active to the Quaternary (Żaba, 1999). All these deep cross-cutting features result in an
338 increased degree of the network connectivity observed on the surface. Then, the blocky structure allowed the
339 formation of an intramountain basin, filled with Neogene sediments.

340

341 Topological analysis also suggests that the well-known Skawa fault zone (Zuchiewicz et al., 2009; Unrug, 1980)
342 is in fact the western-most part of the wider zone of increased network interconnectivity, extending ca. 10–20 km
343 to the west of the Raba River.

344 7. Conclusions

345 The proposed data source and analysis method are complementary with other lineament analysis from the study
346 area. The observed azimuths are in general concordant with the photolineament network; however, there are some
347 structures that are not confirmed by DEM interpretation. The relationship between the DEM-interpreted data and
348 geologically confirmed faults shows the usefulness of DEM as a data source in fault detection.

349 The dominating directions of the network are typical for the Western Carpathians, with a clear increase of the NE
350 striking features proportion towards the east.

351 The topological properties of the lineament network in the Western Carpathians show E–W trends, but no clear
352 S–N (perpendicular to the tectonic units) trends. This justifies the proposed subdivision of the Carpathians in the
353 western, central and eastern sectors in addition to the tectono-facial subdivision. The eastern sectors are dominated
354 by NE–SW trends and low interconnectivity, while the central and western sectors are more interconnected and
355 characterised by cross-cutting relationships of two main lineament directions. The degree of network
356 interconnectivity increases in areas with a lower morphology (intramountainous basins): the Żywiec Basin and
357 Nowy Sącz Basin.

358 The geometry of the network, in general, reflects a system of deep-rooted lineaments. The cross-cutting area of
359 the main deep lineaments is reflected in stronger network interconnectivity in the Nowy Sącz area.

360

361 CRediT authorship contribution statement: Maciej Kania: Conceptualization, Methodology, Formal analysis,
362 Investigation, Writing - original draft, Visualization. Mateusz Szczęch: Investigation, Writing - review &
363 editing, Visualization.

364



365 Declaration of competing interest: The authors declare that they have no known competing financial interests or
366 personal relationships that could have appeared to influence the work reported in this paper
367

368 Acknowledgements: The research was financed from funds of the Jagiellonian University Institute of
369 Geological Sciences. Proofreading of this publication has been supported by a grant from the Priority
370 Research Area (Digiworld) under the Strategic Programme Excellence Initiative at Jagiellonian University.

371 **References**

- 372 Baas, J. H.: EZ-ROSE: a computer program for equal-area circular histograms and statistical analysis of two-
373 dimensional vectorial data, *Comput Geosci*, 26, 153–166, [https://doi.org/10.1016/S0098-3004\(99\)00072-2](https://doi.org/10.1016/S0098-3004(99)00072-2),
374 2000.
- 375 Bażyński, J., Doktor, S., and Graniczny, M.: Mapa fotogeologiczna Polski w skali 1:1 000 000, 1986.
- 376 Chodyń, R.: Zastosowanie cyfrowego modelu terenu (DEM) w badaniach geologicznych na przykładzie obszaru
377 między Dobczycami a Mszaną Dolną (polskie Karpaty zewnętrzne), *Przebieg Geologiczny*, 52, 315–320, 2004.
- 378 Cieszkowski, M., Golonka, J., Waśkowska-Oliwa, A., and Chrustek, M.: Budowa geologiczna rejonu Sucha
379 Beskidzka - Świnna Poręba (polskie Karpaty fliszowe), *Geologia / Akademia Górniczo-Hutnicza im. Stanisława*
380 *Staszica w Krakowie*, 32, 155–201, 2006.
- 381 Cieszkowski, M., Kysiak, T., Szczęch, M., and Wolska, A.: Geology of the Magura Nappe in the Osielec area
382 with emphasis on an Eocene olistostrome with metabasite olistoliths (Outer Carpathians, Poland), *Annales*
383 *Societatis Geologorum Poloniae*, 87, 169–182, <https://doi.org/10.14241/asgp.2017.009>, 2017.
- 384 Danielson, J. J.: Global Multi-resolution Terrain Elevation Data 2010 (GMTED2010) Coastal Elevation
385 Modeling View project LP DAAC View project, 2011.
- 386 Doktor, S. and Graniczny, M.: Geologiczna interpretacja zdjęć satelitarnych i radarowych wschodniej części
387 Karpat, *Kwartalnik Geologiczny*, 26, 231–245, 1982.
- 388 Doktor, S. and Graniczny, M.: Fotogeologiczna analiza zdjęć satelitarnych Karpat, *Kwartalnik Geologiczny*, 27,
389 645–656, 1983.
- 390 Doktor, S., Dornic, J., Graniczny, M., and Reichwalder, P.: Structural elements of Western Carpathians and their
391 Foredeep on the basis of satellite interpretation, *Geological Quarterly*, 29, 129–138, 1985.
- 392 Doktor, S., Graniczny, M., Kucharski, R., Molek, M., and Dąbrowska, B.: Wgłębna budowa geologiczna Karpat
393 w świetle kompleksowej analizy teledetekcyjno-geofizycznej, *Przegląd Geologiczny*, 38, 469–475, 1990.
- 394 Doktor, S., Graniczny, M., Kowalski, Z., and Wójcik, A.: Możliwości zastosowania wyników interpretacji zdjęć
395 radarowych do analizy tektonicznej Karpat, *Przegląd Geologiczny*, 50, 852–860, 2002.
- 396 Ehlen, J.: Lineation, edited by: Goudie, A. S., *Encyclopedia of Geomorphology*, 2, 623–624, 2004.
- 397 Golonka, J., Aleksandrowski Paweł and Aubrecht, R., Chowaniec, J., Chrustek, M., Cieszkowski, M., Florek, R.,
398 Gawęda, A., Jarosiński, M., Kępińska, B., and others: The Orava deep drilling project and post-palaeogene
399 tectonics of the northern Carpathians, *Annales Societatis Geologorum Poloniae*, 75, 211–248, 2005.
- 400 Golonka, J., Waśkowska, A., and Ślącza, A.: The Western Outer Carpathians: Origin and evolution, *Zeitschrift*
401 *der Deutschen Gesellschaft für Geowissenschaften*, 229–254, 2019a.



- 402 Golonka, J., Waškowska, A., and Ślącza, A.: The western outer carpathians: Origin and evolution, *Zeitschrift*
403 *der Deutschen Gesellschaft für Geowissenschaften*, 170, 229–254, <https://doi.org/10.1127/zdgg/2019/0193>,
404 2019b.
- 405 Golonka, J., Gawęda, A., and Waškowska, A.: Carpathians, *Reference Module in Earth Systems and*
406 *Environmental Sciences*, 1–10, <https://doi.org/10.1016/b978-0-12-409548-9.12384-x>, 2020.
- 407 Graniczny, M. and Mizerski, W.: Lineamenty na zdjęciach satelitarnych Polski - próba podsumowania, *Przegląd*
408 *Geologiczny*, 51, 474–482, 2003.
- 409 Kania, M. and Szczęch, M.: Geometry and topology of tectonolineaments in the Gorce Mts. (Outer Carpathians)
410 in Poland, *J Struct Geol*, 141, 104186, <https://doi.org/10.1016/j.jsg.2020.104186>, 2020.
- 411 Kania, M. and Szczęch, M.: Tectonic Structures Interpretation Using Airborne-Based LiDAR DEM on the
412 Examples from the Polish Outer Carpathians, in: *Atlas of Structural Geological and Geomorphological*
413 *Interpretation of Remote Sensing Images*, edited by: Misra, A. A. and Mukherjee, S., 157–165, 2022.
- 414 Książkiewicz, M.: The Tectonics of the Carpathians, in: *Geology of Poland, vol. 4. Tectonics. The Alpine*
415 *Tectonic Epoch*, Geological Institute, Warszawa, 476–608, 1977.
- 416 Leech, D. P., Treloar, P. J., Lucas, N. S., and Grocott, J.: Landsat TM analysis of fracture patterns: A case study
417 from the Coastal Cordillera of northern Chile, *Int J Remote Sens*, 24, 3709–3726,
418 <https://doi.org/10.1080/0143116031000102520>, 2003.
- 419 Lexa, J., Bezák, V., Elečko, M., Mello, J., Polák, M., and Vozár, J.: Geological map of western Carpathians and
420 adjacent areas 1:500 000, 2000.
- 421 Mahel', M.: Tectonics of the Carpathian–Balkan Regions, *Explanations to the Tectonic Map of the Carpathian–*
422 *Balkan Regions and Their Foreland.*, Štátny geologický ústav Dionýza Štúra, Bratislava, 180–197 pp., 1974.
- 423 Marko, F., Andriessen, P. A. M., Tomek, Č., Bezák, V., Fojtíková, L., Bošanský, M., Piovarči, M., and
424 Reichwalder, P.: Carpathian Shear Corridor – A strike-slip boundary of an extruded crustal segment,
425 *Tectonophysics*, 703–704, 119–134, <https://doi.org/10.1016/j.tecto.2017.02.010>, 2017.
- 426 van der Meer, F. D., van der Werff, H. M. A., van Ruitenbeek, F. J. A., Hecker, C. A., Bakker, W. H., Noomen,
427 M. F., van der Meijde, M., Carranza, E. J. M., de Smeth, J. B., and Woldai, T.: Multi- and hyperspectral geologic
428 remote sensing: A review, <https://doi.org/10.1016/j.jag.2011.08.002>, 2012.
- 429 Minár, J., Bielík, M., Kováč, M., Plašienka, D., Barka, I., Stankoviansky, M., and Zeyen, H.: New
430 morphostructural subdivision of the Western Carpathians: An approach integrating geodynamics into targeted
431 morphometric analysis, *Tectonophysics*, 502, 158–174, 2011.
- 432 Motyl-Rakowska, J. and Ślącza, A.: Ważniejsze lineamenty i ich związek ze znanymi, *Przegląd*
433 *Geologiczny*, 32, 72–77, 1984.
- 434 Mukherjee, S.: Using Graph Theory to Represent Brittle Plane Networks, 259–271,
435 <https://doi.org/10.1016/B978-0-12-814048-2.00022-3>, 2019.
- 436 Introducing Esri's Next-Generation Hillshade: [https://www.esri.com/arcgis-blog/products/arcgis-living-](https://www.esri.com/arcgis-blog/products/arcgis-living-atlas/imagery/introducing-esri-next-generation-)
437 [atlas/imagery/introducing-esri-next-generation-](https://www.esri.com/arcgis-blog/products/arcgis-living-atlas/imagery/introducing-esri-next-generation-)



- 438 hillshade/?rmedium=redirect&rsource=blogs.esri.com/esri/arcgis/2014/07/14/introducing-esri-next-generation-
439 hillshade, last access: 1 June 2022.
- 440 Nyberg, B., Nixon, C. W., and Sanderson, D. J.: NetworkGT: A GIS tool for geometric and topological analysis
441 of two-dimensional fracture networks, *Geosphere*, 14, 1618–1634, <https://doi.org/10.1130/GES01595.1>, 2018.
- 442 O’Leary, D. W., Friedman, J. D., and Pohn, H. A.: Lineament, linear, lineation: Some proposed new standards
443 for old terms, *Geological Society of America Bulletin*, 87, 1463–1469, 1976.
- 444 Oszczytko, N.: Late Jurassic-Miocene evolution of the Outer Carpathian fold-and-thrust belt and its foredeep
445 basin (Western Carpathians, Poland), *Geological Quarterly*, 50, 169–194, 2006.
- 446 Ozimkowski, W.: Lineamenty otoczenia Tatr - porównanie interpretacji DEM i MSS, *Przegląd Geologiczny*, 56,
447 1099–1102, 2008.
- 448 Plašienka, D.: Continuity and episodicity in the early Alpine tectonic evolution of the Western Carpathians: How
449 large-scale processes are expressed by the orogenic architecture and rock record data, *Tectonics*, 37, 2029–2079,
450 2018.
- 451 Procter, A. and Sanderson, D. J.: Spatial and layer-controlled variability in fracture networks, *J Struct Geol*, 108,
452 52–65, <https://doi.org/10.1016/j.jsg.2017.07.008>, 2018.
- 453 Sanderson, D. J. and Nixon, C. W.: The use of topology in fracture network characterization, *J Struct Geol*, 72,
454 55–66, <https://doi.org/10.1016/j.jsg.2015.01.005>, 2015.
- 455 Sanderson, D. J., Peacock, D. C. P., Nixon, C. W., and Rotevatn, A.: Graph theory and the analysis of fracture
456 networks, *J Struct Geol*, 14th April, <https://doi.org/10.1016/j.jsg.2018.04.011>, 2018.
- 457 Scheiber, T., Fredin, O., Viola, G., Jarna, A., Gasser, D., and Łapińska-Viola, R.: Manual extraction of bedrock
458 lineaments from high-resolution LiDAR data: methodological bias and human perception, 137, 362–372,
459 <https://doi.org/10.1080/11035897.2015.1085434>, 2015.
- 460 Sikora, W.: On lineaments found in the Carpathians, *Annales de la Société Géologique de France*, 46, 3–37, 1976.
- 461 Ślęczka, A., Kruglov, S., Golonka, J., Oszczytko, N., and Popadyuk, I.: Geology and hydrocarbon resources of
462 the Outer Carpathians, Poland, Slovakia, and Ukraine: general geology, *The Carpathians and their foreland:
463 Geology and hydrocarbon resources: AAPG Memoir*, 84, 221–258, 2006.
- 464 Solon, J., Borzyszkowski, J., Małgorzata Bidłasik, Richling, A., Badora, K., Balon, J., Brzezińska-Wójcik, T.,
465 Chabudziński, Ł., Dobrowolski, R., Grzegorzczak, I., Jodłowski, M., Kistowski, M., Kot, R., Krąż, P., Lechnio,
466 J., Macias, A., Majchrowska, A., Malinowska, E., Migoń, P., Myga-Piątek, U., Nita, J., Papińska, E., Rodzik, J.,
467 Strzyż, M., Terpiłowski, S., Ziaja, W., and Paul, J.: Physico-geographical mesoregions of Poland: verification
468 and adjustment of boundaries on the basis of contemporary spatial data, *Geographia Polonica*, 91, 143–170,
469 <https://doi.org/10.7163/GPol.0115>, 2018.
- 470 Szczęch, M. and Cieszkowski, M.: Geology of the Magura Nappe, south-western Gorce Mountains (Outer
471 Carpathians, Poland), *J Maps*, 17, 453–464, <https://doi.org/10.1080/17445647.2021.1950579>, 2021.
- 472 Teisseyre, W.: O związku w budowie tektonicznej Karpat i ich przedmurza, *Kosmos*, 32, 393–402, 1907.



- 473 Statistics (scipy.stats) — SciPy v1.9.3 Manual: <https://docs.scipy.org/doc/scipy/tutorial/stats.html>, last access: 8
474 November 2022.
- 475 Thiele, S. T., Jessell, M. W., Lindsay, M., Ogarko, V., Wellmann, J. F., and Pakyuz-Charrier, E.: The topology
476 of geology 1: Topological analysis, *J Struct Geol*, 91, 27–38, <https://doi.org/10.1016/J.JSG.2016.08.009>, 2016.
- 477 Unrug, R.: Tectonic rotation of flysch nappes in the Polish Outer Carpathians, *Rocznik Polskiego Towarzystwa*
478 *Geologicznego*, 50, 27–39, 1980.
- 479 Valentini, L., Perugini, D., and Poli, G.: The “small-world” topology of rock fracture networks, *Physica A:*
480 *Statistical Mechanics and its Applications*, 377, 323–328, <https://doi.org/10.1016/j.physa.2006.11.025>, 2007.
- 481 Wójcik, A., Czerwicz, J., and Krawczyk, M.: Szczegółowa Mapa Geologiczna Polski 1:50 000. arkusz
482 Limanowa, 2009.
- 483 Yang, L., Meng, X., and Zhang, X.: SRTM DEM and its application advances,
484 <https://doi.org/10.1080/01431161003786016>, 2011.
- 485 Żaba, J.: Ewolucja strukturalna utworów dolnopaleozoicznych w strefie granicznej bloków górnośląskiego i
486 małopolskiego, *Prace Państwowego Instytutu Geologicznego*, 166, 1–162, 1999.
- 487 Zuchiewicz, W.: The late Neogene - Quaternary tectonic mobility of the Polish West Carpathians - a case study
488 of the Dunajec drainage basin, *Annales Societatis Geologorum Poloniae*, 54, 133–189, 1984.
- 489 Zuchiewicz, W., Tokarski, A. K., Świerczewska, A., and Cuong, N. Q.: Neotectonic Activity of the Skawa River
490 Fault Zone (Outer Carpathians, Poland), *Annales Societatis Geologorum Poloniae*, 79, 67–93, 2009.
- 491
492
493